Filtration of Wastewater via Application of Metal-Organic Frameworks: Model Design, Sensitivity Determination, and Feasibility Study

Brendon Pearlman, Shu Zhu, Yingge Liu

***Abstract*— The purpose of this project is to assess the feasibility of metal-organic frameworks (MOFs) in a wastewater filtration setting. In primary and secondary filtration processes at wastewater treatment facilities throughout the United States, physical separation of debris from used water occurs. To better refine this method of physical separation, inclusion of MOFs for micro- and nano-filtration is proposed as a viable option for optimization of effluent conditions. This study incorporated the Crank-Nicolson finite difference method to visualize a concentration of particles as a function of depth in a given depth filter unit. A sensitivity analysis concluded that diameter of particulate, initial bed porosity, and creep constant are most significant to determining filter performance. Of those parameters, initial bed porosity and creep constant are characteristics of porous media. For proper design of MOFs for inclusion in micro- and nano-filtration, these parameters should be enhanced to achieve feasibility and optimal filter performance.**

I. INTRODUCTION

In the United States, over half of all rivers, streams, and lakes are considered impaired by the Environmental Protection Agency (EPA) [1]. 'Impaired' in this context indicates failure of a body of water to meet one or more water quality standards [2]. These quality standards are classified based on best uses, which range from domestic consumption (Class 1) to Limited Resource Value Water, or LRVW (Class 7). Class 7 waters are so classified because the existing or potential aquatic ecosystem cannot reach aquatic life standards [3]. A contributing factor to the degradation of a body of water is the quality of wastewater being returned to the system. Wastewater is essentially used water - it consists of water from sinks and bathtubs from municipal homes, runoff during storms, and any other substances that may enter waters via human interaction [4].

In the United States, it is estimated that over 14,000 publicly owned wastewater treatment works (POTWs) are continuously operating [1]. These wastewater facilities operate by iteratively addressing the components of wastewater. Initial processing occurs in the form of large-debris physical separation. Generally, this type of filtration makes use of a coarse screen. From primary treatment of large solids, secondary and tertiary treatments consist of clarifications, aeration, and disinfection before producing an effluent (Fig. 1).

After treatment at a POTW or other facility, the effluent is then returned to a nearby waterway. An estimated 255,000 million gallons per day (mgd) of industrial wastewater alone are discharged in the U.S. alone, further emphasizing the scale of wastewater treatment [5]. In the search to optimize primary and secondary filtration of wastewater, metal-organic frameworks may be considered as a feasible option for implementation.

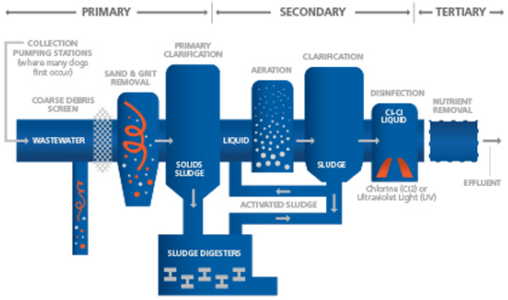

Fig. 1. Typical wastewater treatment process [1]. Used water enters the system on the left and is filtered progressively moving right. Primary filtration consists of solids treatment, while secondary and tertiary filtration focus on chemical clarification and disinfection processes.

A. Metal-Organic Frameworks

In the past several decades, tunable design of metal-organic frameworks has become a popular area of research. MOFs have been found to be an attractive material for myriad technological applications [6]. Because of their high tunability, over 20,000 MOFs have been studied [7]. MOFs are porous systems composed of metal ions linked by organic molecules. In the case of MOF-5, displayed in Fig. 2, Zn_4O tetrahedral molecules are joined together by the organic linker benzene dicarboxylate (BDC). The necessary reaction for formation of MOF-5 is shown in Fig. 3.

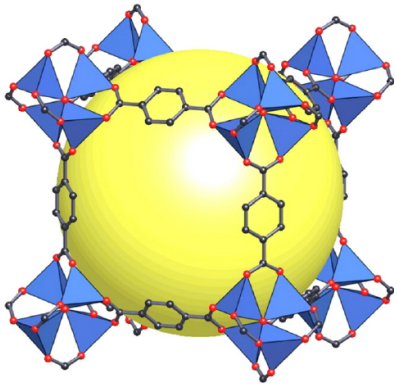

Fig. 2. MOF-5 3-D molecular structure. Zn_4O ions are linked together by the organic molecule benzene dicarboxylate (O: red and C: black) [6].

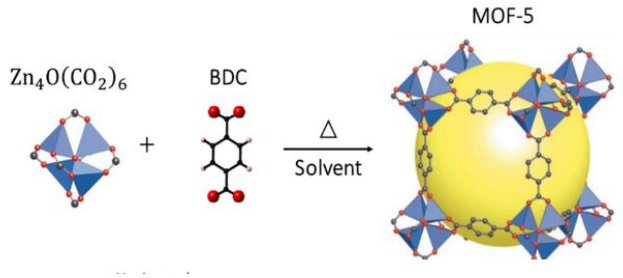

Fig. 3. Reaction of Zn_4O and BDC to form MOF-5. In a large system of MOFs, many organic linkers are used to construct porous media.

Conventionally used for fuel storage, gas adsorption, and catalysis, MOFs are unique in their singular porosity and flexibility [7]. For application in micro- and nano-filtration, one can easily envision tuning structure and porosity of a particular metal-organic framework to optimize filtration performance.

B. Depth Filtration

Depth filtration describes the utilization of a packed bed of porous media to remove suspended filtrate from a fluid through mechanisms including sieving, adsorption, and absorption [8]. Sieving occurs when a particle is larger than the filter media pore size and thereby blocks a pore channel. Through this physical separation method, a cake may develop atop or within the filter. Adsorption, conversely, is a chemical interaction between filtrate and porous media. For adsorption to occur, filtrate must effectively adhere to the filter. This may occur via intermolecular attractions such as Van der Waals force as well as electro-static interactions. In consideration of porous media, pressure drop for incompressible flow is often the parameter for which design is optimized. For creeping flow in which $Re < 1$, Darcy's Law serves as a governing equation for flow characteristics [9, eq. (1)]:

$$\frac{-\Delta P}{L} = \frac{\mu}{k} V \tag{1}$$

Alternatively, Darcy's Law can be expressed in the following manner (eq. (2)):

$$Q = -KA\frac{dh}{dl} \tag{2}$$

where the pressure head is proportional to volumetric flow as well as porous surface area and hydraulic conductivity, which is a measure of the ease with which a fluid moves through a packed pore structure.

II. MODELLING DEPTH FILTRATION

In assessing filter performance, several governing equations are considered. These governing equations characterize suspended particles and their removal from the fluid of import as well as an overall mass balance of the relevant system. Eq. (3) serves as the simplest form of the continuity equation [10]:

$$\frac{\partial}{\partial t}\sigma(t,L) + v\frac{\partial}{\partial L}C(t,L) = 0 \tag{3}$$

Here, one-dimensional, incompressible flow has been assumed. Additionally, diffusivity has been taken as negligible to the system. Observing the changes in particle concentration as a function of filtration time and depth in the filter bed, the following relationship is derived:

$$\frac{\partial C(t,L)}{\partial L} = -\lambda C(t,L) \tag{4}$$

where:

$$\lambda = f(\lambda_0, \sigma(t,L), v(t)) \tag{5}$$

Expanding on the dependencies of the filter coefficient, eq. (6) has been proposed as an appropriate model.

$$\lambda = \lambda_0(v(t)) \left(1+\beta\frac{\sigma_0(t,L)}{\varepsilon_0}\right)^x \left(1-\frac{\sigma_0(t,L)}{\varepsilon_0}\right)^y \left(1-\frac{\sigma(t,L)}{\sigma_u(v(t))}\right)^{z(t)} \tag{6}$$

where:

$$\lambda_0(v(t)) = c_1\frac{S^{1.35}}{v(t)^{0.25}}, \tag{7}$$

$$S = \frac{6(1-\varepsilon_0)}{\psi d_s}, \tag{8}$$

$$\beta = \frac{\alpha}{S^{0.65}}, \tag{9}$$

$$z(v) = c_2\frac{S^{0.61}}{v(t)^{0.24}} \tag{10}$$

In eq. (6), exponents x, y, and z(v(t)) are determined experimentally [10]. As the filter coefficient is dependent upon specific density of the porous media, terms in eq. (6) take into consideration particle deposition on the bed, decreasing bed porosity during filtration, and increasing average filtration velocity due to cake development and decreased area for filtration, respectively.

As a cake develops and suspended particles are deposited onto the porous surface, pressure loss becomes a measurable aspect of filtration. A pressure line equation for a vertical filtration bed is as follows:

$$\frac{\partial}{\partial L}h(t,L) = \frac{\partial}{\partial L}h_0(t,L) - \frac{\partial}{\partial L}h_a(t,L) \tag{11}$$

where:

$$\frac{\partial}{\partial L}h_0(t,L) = \frac{K_0\mu v(1-\varepsilon_0)^2}{\rho g\varepsilon_0^3\psi^2 d_s^2}, \tag{12}$$

$$\frac{\partial}{\partial L}h_a(t,L) = b_1\left(\frac{6(1-\varepsilon_0)^2}{\psi d_s}\right)^{0.9} v^{0.4}\sigma(t,L) \tag{13}$$

The pressure line equation is composed of two main constituents. Eq. (12) serves to consider the initial pressure

loss experienced by flow through a clean filter bed. Meanwhile, eq.(13) accounts for specific head losses due to the concentration of particles and accumulation of particles due to deposition on or within the filter media.

In order to best approximate the particle concentration gradient and assess the change of porous specific density, equation (3) must be solved systematically. This involves the application of partial differential equation (PDE) solving methods, which iteratively solve equations (3), (4), and (6) in order to develop an approximation for the changing absolute specific deposit as a function of time and depth in the bed. Similarly, eq. (11) must be solved through application of PDE solvers.

III. FINITE DIFFERENCE METHOD

Finite difference method (FDM) is a numerical method for solving PDEs by approximating them with difference equations. Time t and depth l can be discretized as follows:

$$t = k\Delta t, k = 0, 1, ..., K-1$$

$$l = i\Delta l, i = 0, 1, ..., I-1$$

where K and I are the number of discrete time and deposit points respectively.

Δt and Δl are the time step and depth step respectively and are defined as follows:

$$\Delta t = T/(K-1)$$

$$\Delta l = L/(I-1)$$

where T and L are total time and depth respectively.

To approximate the unknown solution concentration C(t, l) and the absolute specific deposit σ(t, l), C_i^k and $_i^k$ are used to refer the corresponding discrete point:

$$\frac{\partial C}{\partial L}|_{t=k\Delta t, l=i\Delta l} = \frac{C_i^k - C_{i-1}^k}{\Delta l} \tag{14}$$

$$\frac{\partial \sigma}{\partial t}|_{t=k\Delta t, l=i\Delta l} = \frac{\sigma_i^k - \sigma_{i-1}^k}{\Delta l} \tag{15}$$

Applying to equations:

$$\frac{C_i^k - C_{i-1}^k}{\Delta l} = -\lambda \sigma_i^k C_i^k \tag{16}$$

$$\frac{\sigma_i^k - \sigma_{i-1}^k}{\Delta l} = -v\frac{C_i^k - C_{i-1}^k}{\Delta l} \tag{17}$$

Reorder the above equations:

$$C_i^k - C_{i-1}^k = -\Delta l \lambda \sigma_i^k C_i^k \tag{18}$$

$$\sigma_i^k = \sigma_i^{k-1} + \Delta t v \lambda \sigma_i^{k-1} C_i^{k-1} \tag{19}$$

These two equations make sense for time indices k=1, 2, 3, 4K-1 and depth indices i=1, 2, 3, 4I-1 (on the boundaries):

$$k = 0 : \frac{\sigma_i^0 - \sigma_i^{-1}}{\Delta t} = 0 \tag{20}$$

$$i = 0 : \frac{C_0^k - C_{-1}^k}{\Delta l} = 0 \tag{21}$$

And there are another two boundary conditions:

$$k = K-1 : \frac{\sigma_i^{K-1} - \sigma_i^{K-2}}{\Delta t} = 0 \tag{22}$$

$$i = I-1 : \frac{C_{I-1}^k - C_{I-2}^k}{\Delta l} = 0 \tag{23}$$

Reinterpreting C and in a fixed point in time as vectors:

$$\begin{cases} k = 0 : \sigma_i^0 = \sigma_i^{-1} \\ i = 0 : C_0^k = C_{-1}^k \\ k = K-1 : \sigma_i^{K-1} = \sigma_i^{K-2} \\ i = I-1 : C_{I-1}^k = C_{I-2}^k \end{cases}$$

$$\Rightarrow \begin{cases} C_i^k = \begin{bmatrix} C_0^k \\ \vdots \\ C_{I-1}^k \end{bmatrix} \\ \sigma_i^k = \begin{bmatrix} \sigma_0^k \\ \vdots \\ \sigma_{I-1}^k \end{bmatrix} \end{cases}$$

Rewriting our equations as a linear system:

$$\begin{bmatrix} 0 & 1 & 0 & 0 & 0 & 0 \\ 0 & -1 & 1 & 0 & 0 & 0 \\ 0 & 0 & -1 & 1 & 0 & 0 \\ 0 & 0 & 0 & -1 & 1 & 0 \\ 0 & 0 & 0 & 0 & -1 & 1 \\ 0 & 0 & 0 & 0 & 0 & 0 \end{bmatrix} \begin{bmatrix} C_0^k \\ C_1^k \\ C_2^k \\ \vdots \\ C_{I-2}^k \\ C_{I-2}^k \end{bmatrix} =$$

$$\begin{bmatrix} 0 & 0 & 0 & 0 & 0 & 0 \\ 0 & 0 & 0 & 0 & 0 & 0 \\ 0 & 0 & 0 & 0 & 0 & 0 \\ 0 & 0 & 0 & 0 & 0 & 0 \\ 0 & 0 & 0 & 0 & 0 & 0 \\ 0 & 0 & 0 & 0 & 0 & 0 \end{bmatrix} \begin{bmatrix} C_0^{k-1} \\ C_1^{k-1} \\ C_2^{k-1} \\ \vdots \\ C_{I-2}^{k-1} \\ C_{I-1}^{k-1} \end{bmatrix} - \begin{bmatrix} \Delta l \lambda \sigma_0^k C_0^k \\ \Delta l \lambda \sigma_1^k C_1^k \\ \Delta l \lambda \sigma_2^k C_2^k \\ \vdots \\ \Delta l \lambda \sigma_{I-2}^k C_{I-2}^k \\ \Delta l \lambda \sigma_{I-1}^k C_{I-1}^k \end{bmatrix} \tag{24}$$

$$\begin{bmatrix} 0 & 0 & 0 & 0 & 0 & 0 \\ 0 & 1 & 0 & 0 & 0 & 0 \\ 0 & 0 & 1 & 0 & 0 & 0 \\ 0 & 0 & 0 & 1 & 0 & 0 \\ 0 & 0 & 0 & 0 & 1 & 0 \\ 0 & 0 & 0 & 0 & 0 & 0 \end{bmatrix} \begin{bmatrix} \sigma_0^k \\ \sigma_1^k \\ \sigma_2^k \\ \vdots \\ \sigma_{I-2}^k \\ \sigma_{I-2}^k \end{bmatrix} =$$

$$\begin{bmatrix} 0 & 0 & 0 & 0 & 0 & 0 \\ 0 & 1 & 0 & 0 & 0 & 0 \\ 0 & 0 & 1 & 0 & 0 & 0 \\ 0 & 0 & & 1 & 0 & 0 \\ 0 & 0 & 0 & & 1 & 0 \\ 0 & 0 & 0 & 0 & 0 & 0 \end{bmatrix} \begin{bmatrix} \sigma_0^{k-1} \\ \sigma_1^{k-1} \\ \sigma_2^{k-1} \\ \vdots \\ \sigma_{I-2}^{k-1} \\ \sigma_{I-1}^{k-1} \end{bmatrix} + \begin{bmatrix} \Delta t v \lambda \sigma_i^{k-1} C_i^{k-1} \\ \Delta t v \lambda \sigma_i^{k-1} C_i^{k-1} \\ \Delta t v \lambda \sigma_i^{k-1} C_i^{k-1} \\ \vdots \\ \Delta t v \lambda \sigma_i^{k-1} C_i^{k-1} \\ \Delta t v \lambda \sigma_i^{k-1} C_i^{k-1} \end{bmatrix} \tag{25}$$

The initial condition is $C_0 = 50$ and $\sigma_0 = 0$. Matrices were constructed with numpy.diagflat and the linear system was subsequently solved using numpy.linalg.solve.

This plot shows a similar trend to MATLAB surface plots discussed in Section V.

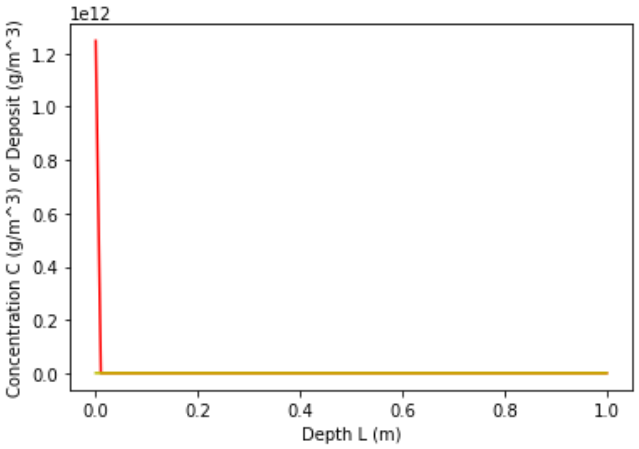

Fig. 4. Concentration C[g/m^3] and deposit [g/m^3] present in the water as a function of depth L[m].

IV. PYTHON IMPLEMENTATION

The filter coefficient λ is a measure of filter performance and is dependent on several parameters. To simplify the PDE, it is reasonable to assume that the filter coefficient is a constant and equal to its initial value:

$$\lambda = \lambda_0 \tag{26}$$

where

$$\lambda_0 = C_1 \frac{S^{1.35}}{v(t)^{2.5}} \tag{27}$$

The assumption yields an ODE:

$$\frac{dC}{dL} = -2.5C \tag{28}$$

Integrating the ODE using odeint from the integration submodule of the scipy package.

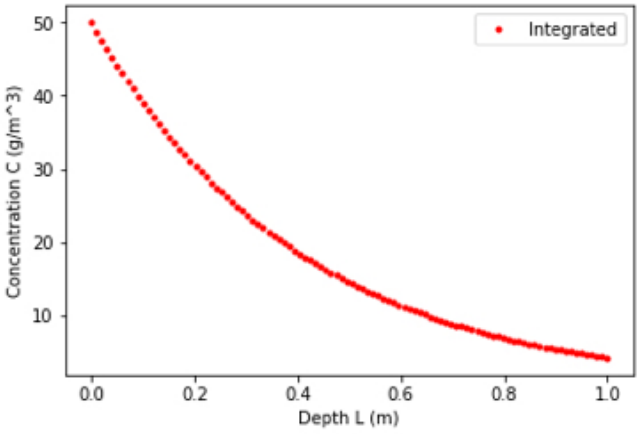

Fig. 5. Mass concentration of particles C[g/m^3] present in the water as a function of depth L[m].

V. MATLAB IMPLEMENTATION

Applying known parameters to equations (6-10) and plugging into eq. (3) and eq.(4), relevant partial differential equations (PDEs) are as follows (note that σ and C remain functions of time t and depth L):

$$\begin{cases} \frac{\partial C}{\partial L} = -0.1\frac{\partial \sigma}{\partial t} \\ \frac{\partial C}{\partial L} = -25C\left(1+\frac{0.05\sigma_0}{2304}\right)^{1.5}\left(1-\frac{\sigma_0}{2304}\right)^{0.75}\left(1-\frac{\sigma}{10000}\right)^{4.8} \end{cases}$$

In MATLAB, the pdepe package can solve PDEs of the form:

$$c\left(x,t,u,\frac{\partial u}{\partial x}\right) = x^{-m}\frac{\partial}{\partial x}\left(x^m f(x,t,u,\frac{\partial u}{\partial x})\right) + s\left(x,t,u,\frac{\partial u}{\partial x}\right)$$

For the system in consideration, the initial condition is of the form:

$$u(x,t_0) = u_0(x)$$

Similarly, the relevant boundary condition can be expressed as:

$$p(x,t,u) + q(x,t)f\left(x,t,u,\frac{\partial u}{\partial x}\right) = 0$$

Applying this methodology to our given PDEs, we obtain

$$\begin{cases} \frac{\partial u_1}{\partial t} = -10\frac{\partial u_2}{\partial x} \\ 0 = -\frac{\partial u_2}{\partial x} + u_2 F \end{cases}$$

where:

$$F = -25C\left(1+\frac{0.05\sigma_0}{2304}\right)^{1.5}\left(1-\frac{\sigma_0}{2304}\right)^{0.75}\left(1-\frac{\sigma}{10000}\right)^{4.8}$$

The given PDE satisfies the initial conditions $u_1(x,0) = 0$ and $u_2(x,0) = 0$. Additionally, it satisfies the following boundary conditions:

- $u_1(0,t) = 50$
- $u_1(0,t) = 0$
- $u_1(1,t) = 0$

To enter the PDEs into MATLAB in the form expected by the pdepe interpreter, the equations become:

$$\begin{bmatrix} 1 \\ 0 \end{bmatrix} \cdot \frac{\partial}{\partial t}\begin{bmatrix} u_1 \\ u_2 \end{bmatrix} = \frac{\partial}{\partial x}\begin{bmatrix} 0 \cdot u_1 \\ -1 \cdot u_2 \end{bmatrix} + \begin{bmatrix} -10 \cdot F \cdot u_2 \\ F \cdot u_2 \end{bmatrix}$$

Accordingly, boundary conditions are reformatted:

$$\begin{bmatrix} u_1 - 50 \\ 0 \end{bmatrix} + \begin{bmatrix} 0 \\ 1 \end{bmatrix}\begin{bmatrix} 0 \cdot u_1 \\ -1 \cdot u_2 \end{bmatrix} = \begin{bmatrix} 0 \\ 0 \end{bmatrix}$$

$$\begin{bmatrix} u_1 \\ 0 \end{bmatrix} + \begin{bmatrix} 0 \\ 1 \end{bmatrix}\begin{bmatrix} 0 \cdot u_1 \\ -1 \cdot u_2 \end{bmatrix} = \begin{bmatrix} 0 \\ 0 \end{bmatrix}$$

Code entered into MATLAB can be found in Appendix C. While rigorous equations were assessed for errors and reviewed repeatedly, surface plots (Fig. 1 and Fig. 2) display unexpected behavior.

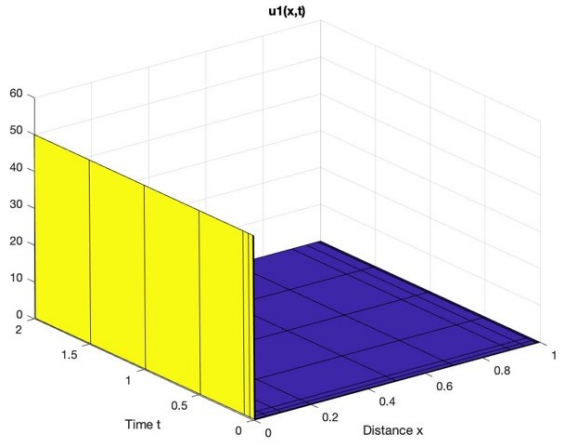

Fig. 6. MATLAB surface plot of suspended particles concentration over time and depth in bed. Behavior shows no change in concentration through the bed.

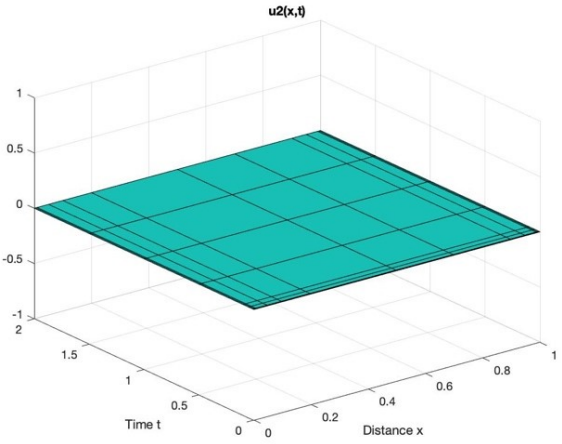

Fig. 7. MATLAB surface plot of absolute specific deposit, σ, as function of time and depth in filter bed.

VI. SENSITIVITY ANALYSIS

A. Preliminary Analysis

In this case study, there are numerous parameters to assess for impact on final outlet concentration of suspended particles in processed wastewater. After simplification of the system of relevance, four parameters are obtained for sensitivity checking:

- Stream Velocity
- Suspended Solids Diameter
- Initial Bed Porosity
- Creep Constant

To begin to assess the impact of each parameter on the outlet particle concentration, Python interaction code was implemented. Fig. 6 shows the Python output allowing for parameters to be manually adjusted. By this method of input, interaction allows impact of various parameters to be visually observed.

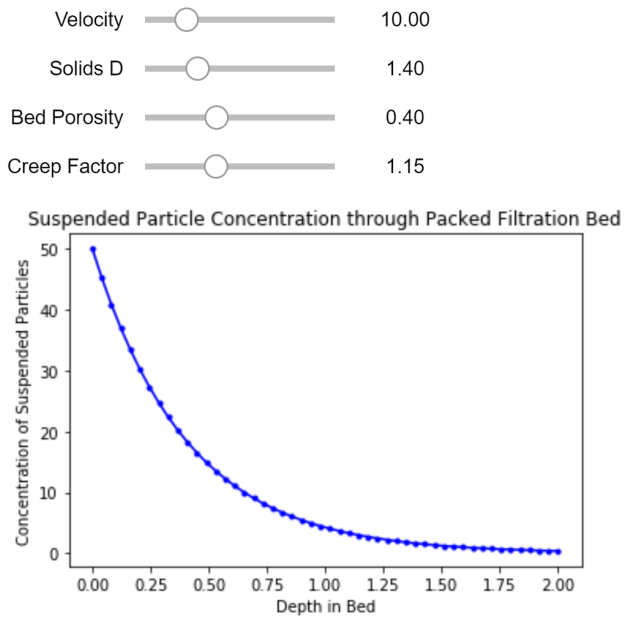

Fig. 8. Python output allowing for live parameter adjustment visualization. Via this method, users may immediately understand how parameters impact desired output.

Following this one-at-a-time method of parameter sensitivity analysis, next steps focused on implementation of a large-scale analysis.

For a sample size of 2000, random numbers were generated for each input to the outlet concentration calculation. A data set was assembled and the random number sets were compared to the overall data output as in Fig. 7.

As Fig. 7 shows, there appears to be a correlation between three of four parameters - solids diameter, initial bed porosity, and creep constant - while stream velocity shows no obvious impact on outlet particle concentration. Progressing to final sensitivity checks, the Sobol analysis technique was implemented.

B. Sobol Sensitivity Analysis

Sobol analysis is performed in order to identify to what extent the variability in a given model is dependent on each input parameter or an interaction between parameters [11]. For the given model, the parameters in Fig. 7 were further analyzed.

Before beginning with a Sobol analysis, the bounds for each parameter must be assessed. The following bounds were used within our analysis:

- Stream velocity: 5.0 - 50 m/h
- Solids diameter: 0.1 - 2.5 mm
- Initial bed porosity: 0.1 - 0.9
- Creep constant: 0.1 - 2.0

Following determination of reasonable bounds for parameters input to the model, analysis may begin. First, parameter sets are generated. For the given scenario, 100,000 values were generated for each of the four parameters. Then, the parameter sets are run through the model and outputs are

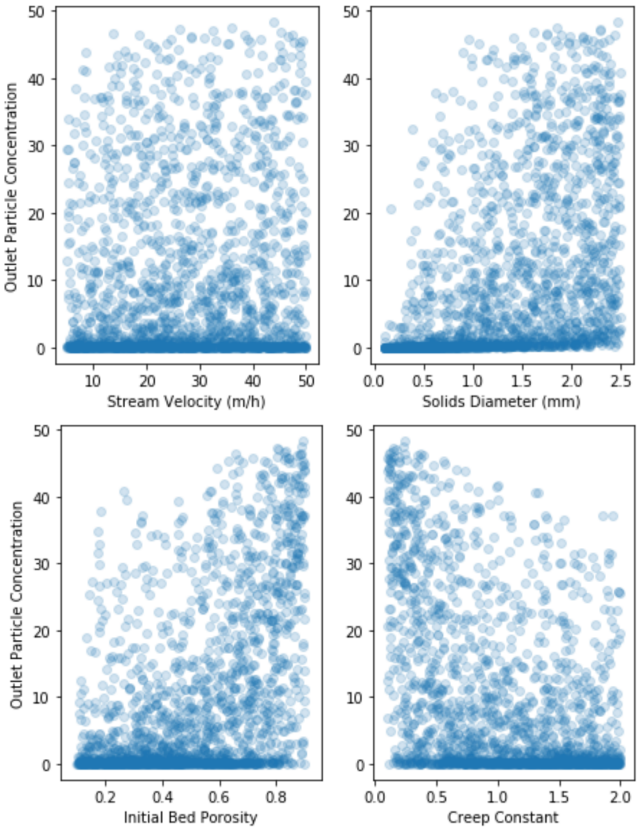

Fig. 9. Output of preliminary sensitivity analysis for 2000 samples performed in Jupyter notebook. Visually, stream velocity has the least significant impact on outlet particle concentration.

recorded. From the 4 x 100,000 array input to the model, a 100,000 x 1 array was returned. With this output, first-, second-, and total-order Sobol sensitivity indices were calculated. The performed analysis output values in Table 1.

TABLE I
SOBOL SENSITIVITY ANALYSIS RESULTS

Name	1st Order	Total	Mean of Input
Velocity	0.007547	0.01428	9.45
Solids Diameter	0.2259	0.3794	1.95
Initial Porosity	0.3177	0.4313	2.083
Creep Constant	0.278	0.3759	1.683

From the Sobol sensitivity analysis output (Table 1), parameters appear to be behaving as expected from output distribution shown in Fig. 7 - solids diameter, initial bed porosity, and creep constant are the most significant parameters. In addition, Table 1 shows that each of those important parameters also have important first-order effects, while stream velocity appears to have more important interaction.

VII. CONCLUSION

In this report, a system capable of modeling filtration efficiency through a porous depth bed was designed by applying known mass balance and continuity equations. Through implementation with both Python and MATLAB, the system was simplified and concentration of suspended particulate was visualized as a function of depth in the filter. From this model output, a sensitivity analysis was performed in order to assess parameter importance in design of filter systems.

Application of a Sobol sensitivity analysis found initial bed porosity and creep constant to be most significant in the effectiveness of a given filter. By optimizing each of these parameters, a filter can ensure optimal effluent conditions. Considering the tunability of metal-organic frameworks, pore size can be adjusted to specifically fit a system. Additionally, the creep constant is a function of porous media. With proper pore sizing and density, creep constant can likewise be tuned to ensure appropriate particulate filtration. This study concludes that application of Python and MATLAB models can be used to understand the necessary structure of an MOF for ideal particulate concentrations in effluent of wastewater. Furthermore, the versatility of metal-organic frameworks will allow for their implementation in wastewater treatment facilities.

VIII. NEXT STEPS

This study found initial bed porosity and creep constant to be the most important parameters to optimize while designing porous media for a given purpose. As metal-organic frameworks have recently been given significant attention, their application to depth filtration is inevitable. To further the potential for MOFs inclusion in filtering processes, this study recommends consideration of stress tolerance and pressure drop capability assessment. By identifying the ability of a given MOF system to withstand high pressures, their application for wastewater treatment will become increasingly feasible.

In addition to delving further into MOF ability to withstand pressure, next steps should include expanding the parameter study to include the filter coefficient and its intrinsic properties (i.e. pore saturation S, porous media resistance β). While this particular study simplified the system to achieve operable conditions, a more rigorous analysis will have fruitful results such as increased parameters for sensitivity analysis.

REFERENCES

[1] Center for Sustainable Systems, University of Michigan. 2018. U.S. Wastewater Treatment Factsheet. Pub. No. CSS04-14. [Accessed: 01- Dec- 2018].
[2] "Water quality standards", Minnesota Pollution Control Agency, 2018. [Online]. [Accessed: 01- Dec- 2018].
[3] C. Anderson, M. Bourdaghs, A. Butzer, D. Duffey, A. Garcia, B. Lundeen, B. Monson, S. Nelson, S. Niemela, D. Oakes and M. Sharp, Thief River Watershed Monitoring and Assessment Report. Saint Paul: Minnesota Pollution Control Agency, 2014, p. 7.
[4] H. Perlman, "Water Use: Wastewater treatment", Water.usgs.gov, 2018. [Online]. [Accessed: 01- Dec- 2018].

[5] "A Look at Wastewater Treatment Processes - Empowering Pumps and Equipment", Empowering Pumps and Equipment, 2018. [Online]. [Accessed: 01- Dec- 2018].
[6] Y. Sun and H. Zhou, "Recent progress in the synthesis of metalorganic frameworks", Science and Technology of Advanced Materials, vol. 16, no. 5, p. 054202, 2015.
[7] H. Furukawa, K. Cordova, M. O'Keeffe and O. Yaghi, "The Chemistry and Applications of Metal-Organic Frameworks", Science, 2013. .
[8] "Depth Filtration, What is it?", ErtelAlsop, 2016. [Online]. [Accessed: 01- Dec- 2018].
[9] H. Van Ness and M. Abbott, Perry's chemical engineers' handbook. [New York]: McGraw-Hill, 2008.
[10] K. Wojciechowska, "Modelling and Simulation of Filtration in the Development of Water Treatment Technologies", Engineering Transactions, vol. 50, no. 4, pp. 323-357, 2002.
[11] X. Zhang, M. Trame, L. Lesko and S. Schmidt, "Sobol Sensitivity Analysis: A Tool to Guide the Development and Evaluation of Systems Pharmacology Models", CPT: Pharmacometrics Systems Pharmacology, vol. 4, no. 2, pp. 69-79, 2015.

SYMBOLS AND ABBREVIATIONS

α	Resistance of porous media
β	Porous media resistance, $1/m$
ε_0	Initial bed porosity
λ	Filter coefficient, $1/m$
μ	Viscosity of fluid containing filtrate
ρ_s	Suspended solids density, g/m^3
σ	Absolute specific deposit, g/m^3
σ_0	Bulk specific deposit, g/m^3
σ_u	Concentration of particles for which the filter coefficient is zero, g/m^3
A	Cross-sectional surface area of filter bed, m^2
C	Suspended particles concentration, g/m^3
c_1	Creep constant
c_2	0.2 $1/m$
c_3	$1.2x10^{-3} - 6.4x10^{-3}$
d_s	Diameter of suspended particles, m
h	Pressure head
K	Hydraulic conductivity
k	Permeability of porous media
L	Depth in Bed, m
l	Depth in bed, m
P	Pressure
Q	Volume flow rate of fluid, m^3/h
S	Pore saturation
v	Stream velocity, m/s
$z(v)$	Average filtration velocity